In Proceedings of NAS Colloquium on Quasars and AGN: High Resolution Radio Imaging, ed. K. I. Kellermann & M. H. Cohen, *Proc. National Acad. Sci.*, in press

PROBES OF THE INNER JETS OF BLAZARS

Alan P. Marscher

Department of Astronomy, Boston University
725 Commonwealth Ave., Boston, MA 02215 USA

Abstract. I review models for the "inner jet" in blazars, the section that connects the central engine with the radio jet. I discuss how the structure and physics of the inner jet can be explored using millimeter-wave VLBI as well as multiwaveband observations of blazars. Flares at radio to γ-ray frequencies should exhibit time delays at different wavebands that can test models for both the high-energy emission mechanisms and the nature of the inner jet in blazars.

INTRODUCTION

Despite our ability to image at sub-milliarcsecond resolution the radio jets of blazars (defined as BL Lacertae objects and quasars with strong, highly variable nonthermal emission), we are still ignorant of some of the most important aspects of these jets. We do not know how or where the jets are formed, accelerated to flow speeds near that of light, and collimated into cones of very small ($1 - 5°$) opening angles. Nor do we understand well the process by which the ultrarelativistic, magnetized plasma in a jet is generated or how the radiating electrons are re-accelerated downstream of the source of the jet. All of these processes must occur in the region that I refer to as the "inner jet," which is the portion of the jet that lies between the central engine and the core of the radio jet observed with very-long baseline interferometry (VLBI). In what follows, I review the major models for the inner jet and discuss how we can test these models using current observational techniques.

THE CORE AND INNER JET

The VLBI core is the compact, flat-spectrum component that lies at one end of the centimeter-wave radio image of a typical blazar. Theoretically, the core is the narrow end of the undisturbed jet flow, while the knots that appear to separate from the core at superluminal velocities are propagating disturbances such as shock waves[1]. The core is therefore a stationary feature, although the plasma flows through it at speeds near that of light. At centimeter wavelengths, the cores of blazars are optically thick to synchrotron self-absorption.

The total synchrotron spectrum of the jet at radio frequencies is quite flat. This is caused by a superposition of the spectrum of the core and the knots that lie downstream in the jet. The principle is illustrated in Figure 1, which is a sketch of how the flat spectrum of the entire compact jet is formed by the individual sections of the jet. As one considers ever more compact regions closer to the origin of the jet, the spectrum from each successive section peaks at a progressively higher frequency. The flat total spectrum can be obtained if the magnetic field in the jet falls off as R^{-1} and the normalization to the relativistic electron energy distribution varies as R^{-2}, where R is the distance from the origin[2]. It can also result from radiative losses behind the shock fronts in models in which such shocks are identified as superluminal knots[3]. The size of a component should be inversely proportional to the peak frequency of its spectrum, as is generally observed.

Figure 1 illustrates another important point: the jet cannot be self-similar down to extremely small size scales, otherwise the total spectrum would remain flat well beyond the observed turnover at (typically) $10^{11\pm0.5}$ Hz. The angular sizes of the radio cores tend to be of order 0.1 milliarcseconds at frequencies of several tens of GHz, so at the turnover frequency of $10^{11\pm0.5}$ Hz, we expect the sizes to be ~ 0.01 to 0.1 milliarcseconds. For a Hubble constant $H_0 = 100h$ km s^{-1} Mpc^{-1}, this translates to a linear

size ranging from $\sim 4 \times 10^{16\pm0.5}h^{-1}$ cm at a redshift $z = 0.03$ to $\sim 4 - 5 \times 10^{17\pm0.5}h^{-1}$ cm at $z = 2$ (for a deceleration parameter q_0 between 0.5 and 0.1). This refers to the *width* of the jet, which has an opening angle of only a few degrees. Hence, the distance from the central engine is likely to be roughly an order of magnitude greater than the estimated size of the radio core given above. Therefore, *either the jet forms at a considerable distance — as great as* ~ 1 *parsec* (3×10^{18} *cm) — from the central engine, or the jet ceases to be self-similar at the position of the VLBI core.*

These two options form the basis of the inner jet models that have been proposed. In the earliest version[4,5], the jet accelerates hydrodynamically from a de Laval nozzle as described by Blandford and Rees[6]. (It is thought that an initial collimation, for example by magnetic focussing, is also required; see Begelman's paper in these proceedings.) As the internal energy of the plasma is converted into kinetic energy of bulk flow, the Lorentz factor of the jet increases. The VLBI core is then the site where the Lorentz factor reaches its maximum value as the internal energy becomes nonrelativistic (i.e., rest-mass dominated). The final bulk Lorentz factor equals the initial internal energy per unit rest mass (minus any that is lost through radiation). The inner jet is detected at higher frequencies, with the synchrotron spectrum becoming progressively steeper toward optical and (for many BL Lac objects) X-ray frequencies. An alternative is the proposal[7] that the central engine produces a highly directed, ultrarelativistic electron-positron beam that scatters photons produced outside the jet. This scattering produces X-rays and γ-rays while the recoil causes the beam to decelerate and become a plasma with random internal motions in addition to a residual bulk flow with Lorentz factor ~ 10.

Three further models for the inner jet call for the generation of the radiating particles to occur well downstream of the origin of the jet, at the VLBI core. They are therefore rather independent of the details of jet formation and initial particle acceleration. In the proton[8] or electron[9] initiated pair cascade models, relativistic electron-positron pairs are produced through interactions of the ambient photon field in the blazar and subsequent particle cascade. In the neutron-decay model[10,11], an ultrarelativistic neutron beam is emitted by the central engine as the result of hadron collisions. The neutrons then decay at a distance downstream that is lengthened from the proper value of $\sim$ 1000 light-seconds via relativistic time dilation. The neutrons decay into protons and electrons, which become a relativistically flowing plasma after interacting with the ambient medium. The final model[12] of this type re-energizes a jet that was visible only at small radii via a standing shock wave.

TESTING THE INNER JET MODELS

The models sketched above make different predictions that can be tested observationally. The most straightforward test is to image directly the inner jet through VLBI observations at frequencies where the core is optically thin. Since VLBI can now produce images at 90 GHz, which is above the turnover frequency for a number of blazars, this should be possible. Figure 2 sketches the intensity profiles (expressed in the practical units of flux density per unit length along the jet) expected according to various models.

Another major test is to observe nonthermal flares at a wide range of frequencies. As is illustrated in Figure 3 for the accelerating and decelerating jet models, the relative positions of the primary sites of radiation at each waveband are quite model dependent. Flares should therefore exhibit frequency-dependent time delays. Since there are a number of versions of each model, listing the specific predictions of each is beyond the scope of this brief review; the reader is referred to a previous review[13] of γ-ray emission from blazars.

Over 40 blazars have been detected[14] at γ-ray frequencies by the high-energy EGRET detector of the *Compton* Gamma Ray Observatory. In these cases the γ-rays dominate the apparent nonthermal luminosities of the blazars. The most successful models to this date generate the γ-rays through inverse Compton scattering off the relativistic electrons in the jet[13]. However, it is not yet clear whether the "seed" photons are synchrotron radiation from the jet (synchrotron self-Compton scattering[15], or SSC), direct photons from the putative accretion disk[7,16], or photons originally from the central engine that have been scattered nonrelativistically in the ambient medium[17,9].

The continued operation of EGRET therefore provides an excellent opportunity to explore the physics of the inner jets of blazars, especially if γ-ray flares can be observed simultaneously at other wavebands. There are a number of such campaigns, with results that are starting to be published. Although much

remains to be learned from these studies, the following findings already provide important information:

1. The γ-ray emission is bright when the overall multiwaveband emission is in a high state[18]. The ratio of γ-ray to X-ray luminosity is higher than the ratio of X-ray to IR luminosity, contrary to the predictions of models in which the γ-ray emission is second-order self-Compton scattering[19], thereby eliminating that model. Only first-order scattering is viable.
2. Flares observed by EGRET have lower-frequency counterparts. In 1406-076, an optical flare[20] preceded by one day a γ-ray flare in January 1992. This implies that the γ-rays are produced farther down the jet than is the optical emission. In the accelerating jet model[21] (see Fig. 3) the γ-rays would then be inverse Compton scattered IR photons, since these are produced slightly farther down the jet than are the optical photons in inhomogeneous jet models. (In non-SSC models, the one-day delay seems more difficult to explain.) In PKS 0528+134 the high-amplitude γ-ray flare of March 1993 occurred near the peak of a months-long mm-wave flare[22]. This supports the SSC model, which predicts a nonlinear response of the γ-rays to synchrotron variations. This nonlinear response is also seen in the two multiwaveband "snapshots" of June 1991 and Dec-Jan 1992-3[18]. However, inverse Compton scattering of seed photons produced outside the jet could also show such a nonlinear response if the Lorentz factor of the jet flow were time-variable.
3. The γ-ray flare of Mkn 421 observed at TeV photon energies by the Whipple Observatory in May 1994 was simultaneous with an X-ray flare but there was little change in the EGRET, mm-wave, IR, or uv emission[23]. In this case the flare seems to have resulted from an increase only in the efficiency of acceleration of the highest energy electrons (the "tail" of the electron energy spectrum). These observations appear to disprove the pair cascade models for this source, but are in concert with the model in which nonthermal flares are caused by shock waves in the jet[3].
4. In two objects (0528+134 and 3C 279), new superluminal components observed with VLBI were created near the times of γ-ray flares and at the beginning of mm-wave rises[24,25]. The flares therefore appear to be associated with the production of new knots that flow down the jet.
5. The γ-ray variability of a few days observed in some blazars requires relativistic beaming in order to avoid high optical depths to photon-photon pair production that would prevent the γ-rays from escaping. The Lorentz factors implied are similar to those needed to explain apparent superluminal motion in blazars[26].

CONCLUSION

The inner jet is the most important yet most poorly understood region of relativistic jets. We can claim truly to understand galactic nuclei only when we have successfully explained how these exotic jets arise in so many cases. The recent availability of mm-wave VLBI imaging and X-ray and γ-ray telescopes with sufficient sensitivity to detect flares in blazars will provide us with a wealth of information that, in concert with other types of observations, should soon lead to more refined models for the physics of the inner jets. This will guide us in our effort to deduce the nature of the central engine that powers energetic activity in the hearts of galaxies.

ACKNOWLEDGMENTS

This review is based upon research supported in part by the National Science Foundation through grant AST-9116525 and by NASA through grant NAG5-2508.

REFERENCES

1. Blandford, R. D. & Königl, A. (1979) *Astrophys. J.* **232**, 34–48.
2. Königl, A. (1981) *Astrophys. J.* **243**, 700–709.
3. Marscher, A. P. & Gear, W. K. (1985) *Astrophys. J.* **298**, 114–127.
4. Reynolds, S. P. (1982) *Astrophys. J.* **256**, 13–27.
5. Marscher, A. P. (1980) *Astrophys. J.* **235**, 386–391.
6. Blandford, R. D. & Rees, M. J. (1974) *Mon. Not. Royal Astron. Soc.* **169**, 395–415.

7. Melia, F. & Königl, A. (1989) *Astrophys. J.* **340**, 162–180.
8. Mannheim, K. (1993) *Astron. & Astrophys.* **269**, 67–76.
9. Blandford, R. D. & Levinson, A. (1995) *Astrophys. J.* **441**, 79–95.
10. Eichler, D. & Wiita, P. J. (1978) *Nature* **274**, 38–39.
11. Giovanoni, P. M. & Kazanas, D. (1990) *Nature* **345**, 319–322.
12. Marscher, A. P. & Daly, R. A. (1988) *Astrophys. J.* **334**, 539–551.
13. Marscher, A. P. & Bloom, S. D. (1994) in *The Second Compton Symposium*, eds. Fichtel, C., Gehrels, N., & Norris, J. P., *Amer. Inst. Phys. Conf. Proc.* **304**, pp. 572–581.
14. von Montigny, C., *et al.* (1995) *Astrophys. J.* **440**, 525–553.
15. Jones, T. W., O'Dell, S. L., & Stein, W. A. (1974) *Astrophys. J.* **188**, 353–368.
16. Dermer, C. D., Schlickeiser, R., & Mastichiadis, A. (1992) *Astron. & Astrophys.* **256**, L27–L30.
17. Sikora, M., Begelman, M. C., & Rees, M. J. (1994) *Astrophys. J.* **421**, 153–162.
18. Maraschi, L., Ghisellini, G., & Celotti, A. (1992) *Astrophys. J.*, **397**, L5–L9.
19. Jones, T. W. (1979) *Astrophys. J.*, **233**, 796–798.
20. Wagner, S. J. (1995) in *17th Texas Symposium on Relativistic Astrophysics* (New York: NY Academy of Sciences), in press.
21. Maraschi, L., *et al.* (1994) *Astrophys. J.*, **435**, L91–L95.
22. Zhang, Y. F., Marscher, A. P., Aller, H. D., Aller, M. F., Teräsranta, H., & Valtaoja, E. (1994) *Astrophys. J.* **432**, 91–102.
23. Macomb, D., *et al.* (1995) *Astrophys. J.*, in press.
24. Pohl, M., *et al.* (1995) *Astron. & Astrophys.*, in press.
25. Wehrle, A. E., Zook, A. C., Unwin, S. C., Urry, C. M., & Gilmore, D. (1994) *Bull. Amer. Astron. Soc.*, **26**, 1507 (Abstract).
26. Mattox, J. R., *et al.* (1993) *Astrophys. J.*, **410**, 609–614.

FIGURE CAPTIONS

Fig. 1.— Sketch of the synchrotron spectrum of a self-similar relativistic jet, in arbitrary units. The top panel shows the section of the jet that corresponds to each spectrum in the bottom panel. The flat part of the total spectrum (bold curve) would continue to higher frequencies were the jet to remain self-similar to the left of section D.

Fig. 2.— Flux density per unit length of relativistic jets according to various models. The curves are either qualitative or quantitative but for selected values of free parameters inside of the core, which is arbitrarily given a distance from the origin $R = 10^{18}$ cm. Solid curve: slowly accelerating jet model; dashed curve: more rapidly accelerating jet model; dash-dot curve: invisible inner jet becomes progressively brighter with increasing R, as expected according to the decelerating jet model or particle cascade models; dotted curve: invisible inner jet made abruptly visible by a standing shock at the position of the VLBI core. All models have similar behavior beyond $R = 10^{18}$ cm.

Fig. 3.—Top panel: tapered, accelerating jet model[5,18]. The density of dots in the jet corresponds roughly to the emissivity of the synchrotron radiation. Bottom panel: decelerating jet model[7]. Compton "reflection" of accretion disk photons by the relativistic particle beam decelerates the beam, which becomes the observed radio jet. For both models, the regions of emission at different wavebands are indicated, and the lengths of the arrows roughly indicate on a logarithmic scale the Lorentz factor of the flow.

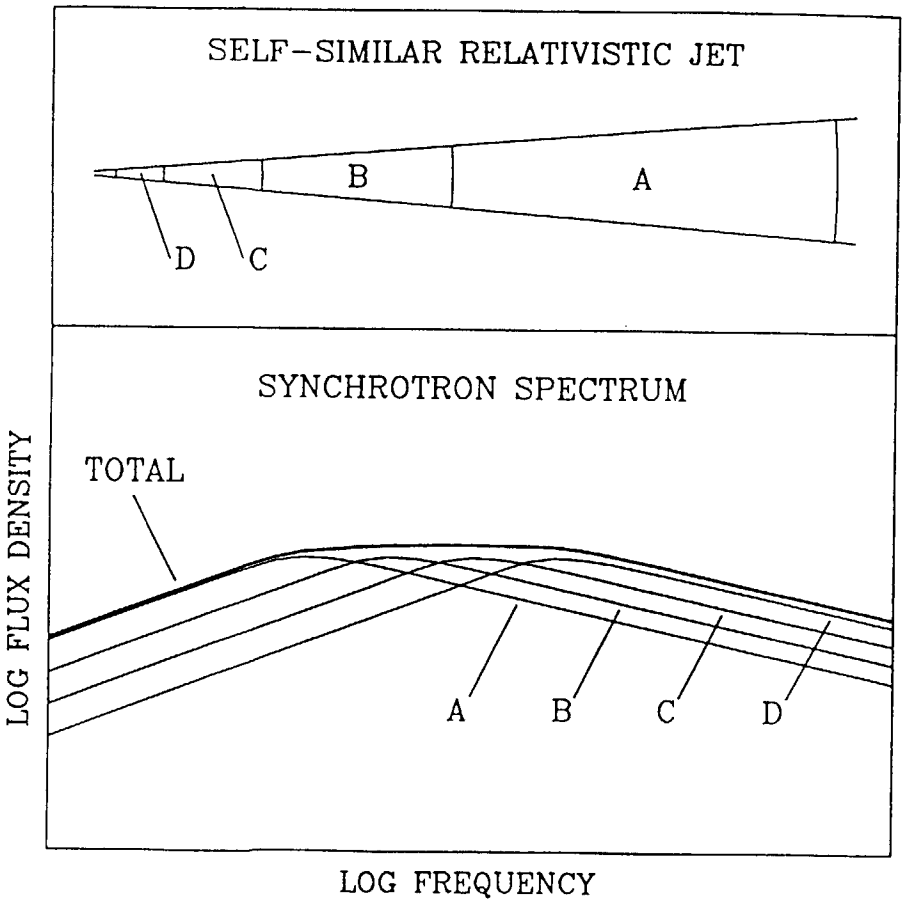
SELF-SIMILAR RELATIVISTIC JET
B
A
D
C
SYNCHROTRON SPECTRUM
TOTAL
A
B
C
D
LOG FLUX DENSITY
LOG FREQUENCY

Fig. 1

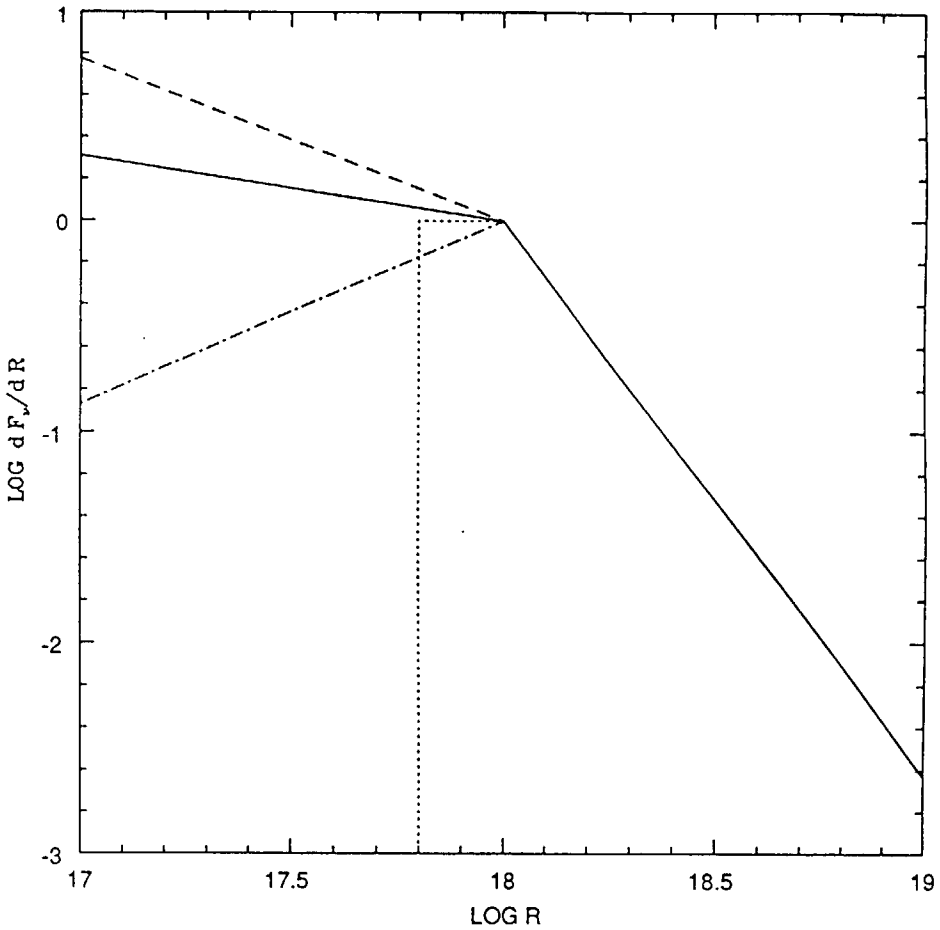
1
0
-1
-2
-3
17
17.5
18
18.5
19
LOG dF$_\nu$/dR
LOG R

Fig. 2

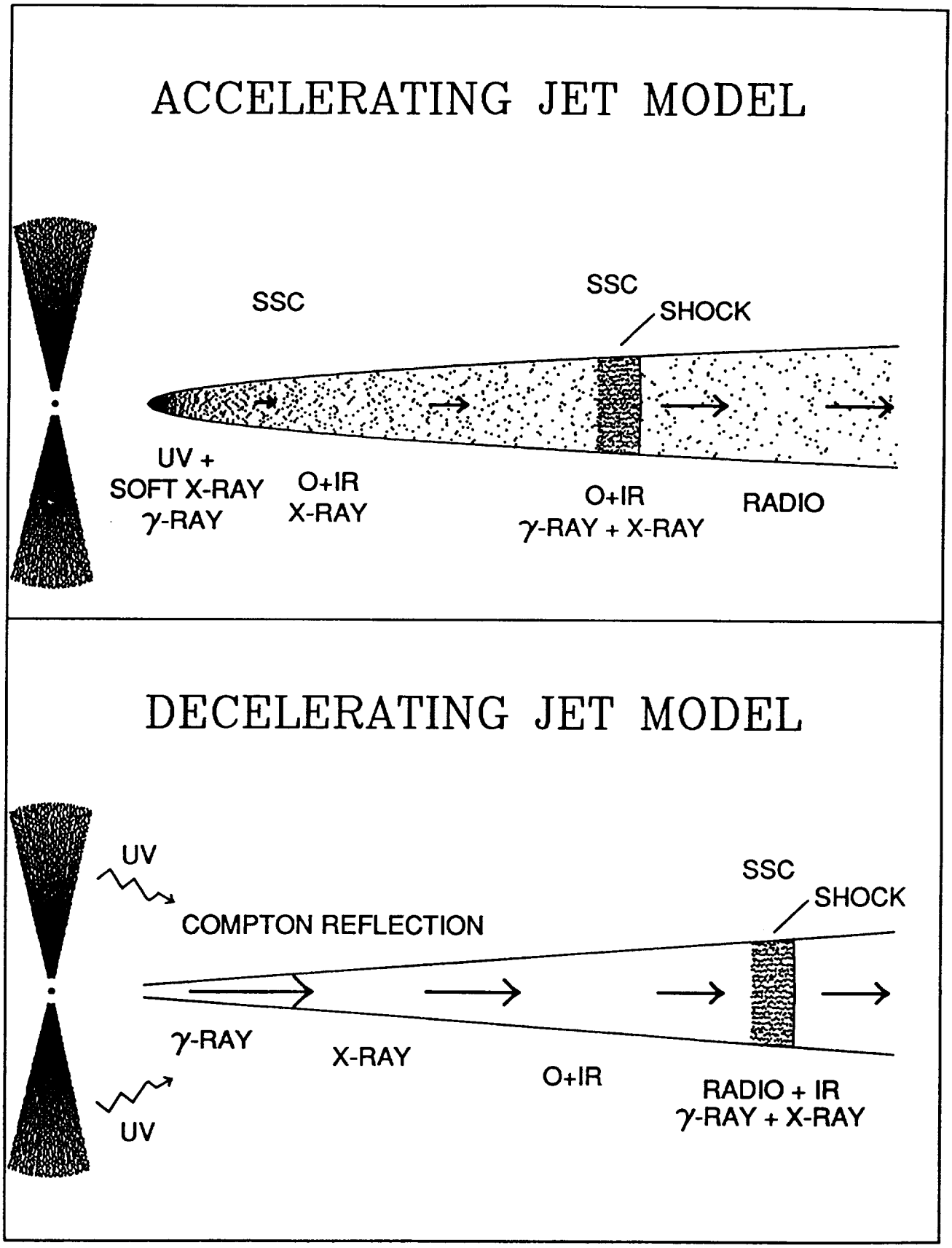
ACCELERATING JET MODEL
SSC
SSC
SHOCK
UV +
SOFT X-RAY
γ-RAY
O+IR
X-RAY
O+IR
γ-RAY + X-RAY
RADIO
DECELERATING JET MODEL
UV
COMPTON REFLECTION
SSC
SHOCK
γ-RAY
X-RAY
O+IR
RADIO + IR
γ-RAY + X-RAY
UV

Fig. 3